



## Satellite-derived, melt-season surface temperature of the Greenland Ice Sheet (2000–2005) and its relationship to mass balance

D. K. Hall,<sup>1</sup> R. S. Williams Jr.,<sup>2</sup> K. A. Casey,<sup>3</sup> N. E. DiGirolamo,<sup>3</sup> and Z. Wan<sup>4</sup>

Received 28 March 2006; revised 27 April 2006; accepted 2 May 2006; published 8 June 2006.

[1] Mean, clear-sky surface temperature of the Greenland Ice Sheet was measured for each melt season from 2000 to 2005 using Moderate-Resolution Imaging Spectroradiometer (MODIS)-derived land-surface temperature (LST) data-product maps. During the period of most-active melt, the mean, clear-sky surface temperature of the ice sheet was highest in 2002 ( $-8.29 \pm 5.29^\circ\text{C}$ ) and 2005 ( $-8.29 \pm 5.43^\circ\text{C}$ ), compared to a 6-year mean of  $-9.04 \pm 5.59^\circ\text{C}$ , in agreement with recent work by other investigators showing unusually extensive melt in 2002 and 2005. Surface-temperature variability shows a correspondence with the dry-snow facies of the ice sheet; a reduction in area of the dry-snow facies would indicate a more-negative mass balance. Surface-temperature variability generally increased during the study period and is most pronounced in the 2005 melt season; this is consistent with surface instability caused by air-temperature fluctuations. **Citation:** Hall, D. K., R. S. Williams Jr., K. A. Casey, N. E. DiGirolamo, and Z. Wan (2006), Satellite-derived, melt-season surface temperature of the Greenland Ice Sheet (2000–2005) and its relationship to mass balance, *Geophys. Res. Lett.*, 33, L11501, doi:10.1029/2006GL026444.

### 1. Introduction

[2] Extensive, perhaps historically unprecedented melt has occurred on the Greenland Ice Sheet in the last 25 years as determined from ground, aircraft and satellite data [Abdalati and Steffen, 1995, 2001; Krabill et al., 2000; Nghiem et al., 2001; Comiso et al., 2003; Steffen et al., 2004; Rignot and Kanagaratnam, 2006] (see also K. Steffen and R. Huff, <http://cires.colorado.edu/science/groups/steffen/greenland/melt2005/>). Analysis of snow-melt extent using passive-microwave satellite data showed that the maximum melt area increased 16% from 1979–2002 [Steffen et al., 2004]. Both surface and subsurface melt are detected with passive-microwave data and while both are important in meltwater production, most of the subsurface melt refreezes close to where it was formed [e.g., see Joshi et al., 2001]. However surface melt, which is directly related to surface temperature, may contribute more directly

to accelerated disintegration of the ice sheet because of its rapid movement to the base of the ice sheet where it can allow accelerated ice flow, leading to sea-level rise [Zwally et al., 2002].

[3] The importance of monitoring surface temperature is highlighted by recent modeling studies showing that summer temperature increases of only  $\sim 2\text{--}5^\circ\text{C}$  are required to double melt rates and thus increase runoff from the Greenland Ice Sheet [Hanna et al., 2005]. To assess interannual surface-temperature variability across Greenland, we analyze clear-sky surface temperature of the ice sheet derived from Moderate-Resolution Imaging Spectroradiometer (MODIS) land-surface temperature (LST) standard-data product maps for six melt seasons (2000–2005), and relate the results to ice-sheet mass balance.

### 2. Background

[4] Carl Benson's pioneering work on the Greenland Ice Sheet led to his classification of the ice sheet into an ablation area and an accumulation area, separated by the equilibrium line where the net mass balance equals zero [Benson, 1962]. Various facies exist within the accumulation area, the approximate boundaries of which may sometimes be identified by their unique spectral signatures [Hall et al., 1989; Williams et al., 1991; Fahnestock et al., 1993; Abdalati and Steffen, 1995; Long and Drinkwater, 1999]. The facies boundaries change over time with changes in the ice-sheet mass balance. For example, the dry-snow area may shrink if the mass balance becomes more negative over a period of years.

[5] Surface-temperature conditions on the Greenland Ice Sheet have been studied extensively [e.g., Key and Haefliger, 1992; Haefliger et al., 1993; Shuman et al., 2001; Steffen and Box, 2001; Comiso et al., 2003]. Using Advanced Very-High Resolution Radiometer data, Stroeve and Steffen [1998] derived surface temperatures over Greenland from 1989 to 1993. Monthly mean summer ice-sheet temperatures showed little variation between years, though they cited 1992 as having lower monthly-mean temperatures than the other years due to the worldwide cooling related to the eruption of Mt. Pinatubo. Comiso et al. [2003] measured increased AVHRR-derived surface temperatures in the Arctic poleward of  $60^\circ\text{N}$ , beginning in 1981.

### 3. Data and Methodology

[6] MODIS LST data products consist of daily and 8-day composite 1-km and  $0.05^\circ$ -resolution map products, with quality-control information in each 1-km pixel or  $0.05^\circ$  cell. We selected the 8-day composite  $0.05^\circ$ -resolution product (MOD11C2) to use for this work because the maps provide

<sup>1</sup>Cryospheric Sciences Branch, NASA Goddard Space Flight Center, Greenbelt, Maryland, USA.

<sup>2</sup>U.S. Geological Survey, Woods Hole Science Center, Woods Hole, Massachusetts, USA.

<sup>3</sup>Science Systems and Applications, Inc., Lanham, Maryland, USA.

<sup>4</sup>Institute for Computational Earth System Science, University of California, Santa Barbara, California, USA.

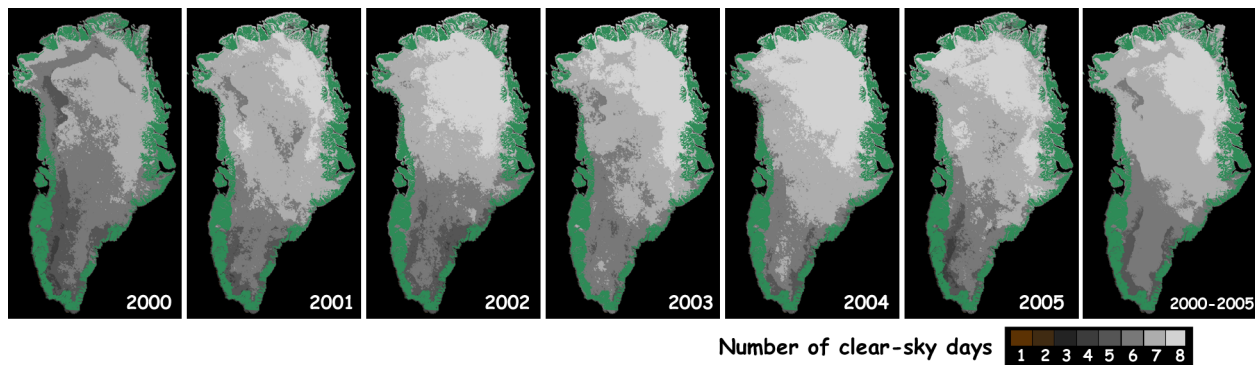


**Figure 1.** Maps showing average number of clear-sky days within each 8-day period during the melt season of each year, derived from the MOD11C2 land-surface temperature (LST) map product on a cell-by-cell basis. The melt season is defined to extend from April 30 or May 1 to September 28 or 29 (days 121–272).

an 8-day average LST for each cell (cloud-cover permitting). MOD11C2 is derived from the 1-km and 0.05°-resolution daily products [Wan *et al.*, 2002].

[7] Temperatures derived from the daily, 1-km LST product have been compared with in-situ measurements using multiple thermal-infrared radiometers in field campaigns including one in a snow field, where the error was generally  $<1^{\circ}\text{C}$  [Wan *et al.*, 2002], but could get up to  $2^{\circ}\text{C}$ . Furthermore, the LST is relatively constant, between  $-2^{\circ}$  and  $0^{\circ}\text{C}$ , in the exposed ice region within the ablation area of the Greenland Ice Sheet, and the LST does not exceed  $0^{\circ}\text{C}$  over ice with surface melt.  $0^{\circ}\text{C}$  represents the upper boundary of LST for the glacier ice and is consistent with the expected temperature of melting ice. The automatic weather-station (AWS) data on the Greenland Ice Sheet [Steffen and Box, 2001] are useful in checking the trend of seasonal variations in MODIS LST data with surface air temperature or upper-level snow temperature profile data, however it is difficult to use these data to compare directly with the values in the LST product because there is no accurate radiometric measurement of snow-surface temperature in the AWS data.

[8] The major uncertainty in the LST product is the effect of cloud contamination because it is often difficult to discriminate cloud-contaminated from clear-sky LSTs over snow and ice in cold regions, especially in the case of thin clouds or fog that may not be detected by the MODIS cloud mask. The MODIS LST algorithm uses a cloud mask derived from MODIS data [Ackerman *et al.*, 1998] to determine whether or not to calculate LST. The cloud mask tends to be conservative, generally mapping more clouds than are actually present over snow and ice.

[9] MODIS maps provide LST only when the sky is clear, causing a bias because surface temperatures are generally warmer under clouds, especially low clouds (K. Steffen, personal communication, 2005). (The air temperature difference between an overcast and clear day can be several  $^{\circ}\text{C}$ .) Thus the “mean” clear-sky LSTs represent a likely underestimation of the actual mean-surface temperatures.

[10] In some cases there is only one clear day available to create the 8-day LST map for any given cell, thus the LST of each cell may not represent a true mean for the 8-day period. Figure 1 shows the average number of clear-sky

days for each 8-day period during the entire melt season [defined as extending from April 30 or May 1 (depending on whether or not it was a leap year) (day 121) to September 28 or 29 (day 272) of each year]. Data used in Figure 1 were derived from the MODIS LST MOD11C2 product, and provide an indication of the relative cloudiness among the years.

[11] Nineteen 8-day-mean LST maps of Greenland were averaged on a cell-by-cell basis for the entire melt season (between days 121 and 272), to develop one map of mean-surface temperature along with a standard deviation (SD) map for each melt season. (Only 17 and 18 maps were used for 2001 and 2004, respectively, due to missing and/or suspected-bad data.) In addition, we also studied the period of most-active melt in each year, May through mid-August [days 121 to 225 (August 12 or 13)]. Because freezeup can begin around mid-August, we consider days 121–225 to be the period of most-active melt for the purpose of this work. Surface temperatures during the most-active part of the melt season are more relevant to surface melt on the ice sheet than those derived from the entire melt season, during which time subsurface melt may play a significant role.

#### 4. Results

[12] Mean, clear-sky surface temperature with SD for each melt season is shown in Figure 2 and Table 1. The mean, clear-sky surface temperature of the entire melt seasons for the six years is  $-10.71 \pm 6.66^{\circ}\text{C}$ . The highest mean LST for the entire melt season,  $-9.94 \pm 6.19^{\circ}\text{C}$ , occurred in 2002. According to the two-tailed z-test, the probability is  $>99.999\%$  that the difference between the mean, clear-sky surface temperatures for 2002, and each of the other years, is statistically significant.

[13] The surface temperature was highest,  $-8.29^{\circ}\text{C}$ , in both 2002 and 2005 during the period of most-active melt (Table 1). This is  $0.75^{\circ}\text{C}$  higher than the 6-year mean,  $-9.04 \pm 5.59^{\circ}\text{C}$ , for this time period.

[14] The SD maps in Figure 2 show that the surface-temperature variability tends to be greater in the northern part of the ice sheet and increases throughout the study period. This is related to increasing air-temperature fluctuations, leading to surface instability. There is evidence of increasing ice discharge from outlet glaciers in recent years

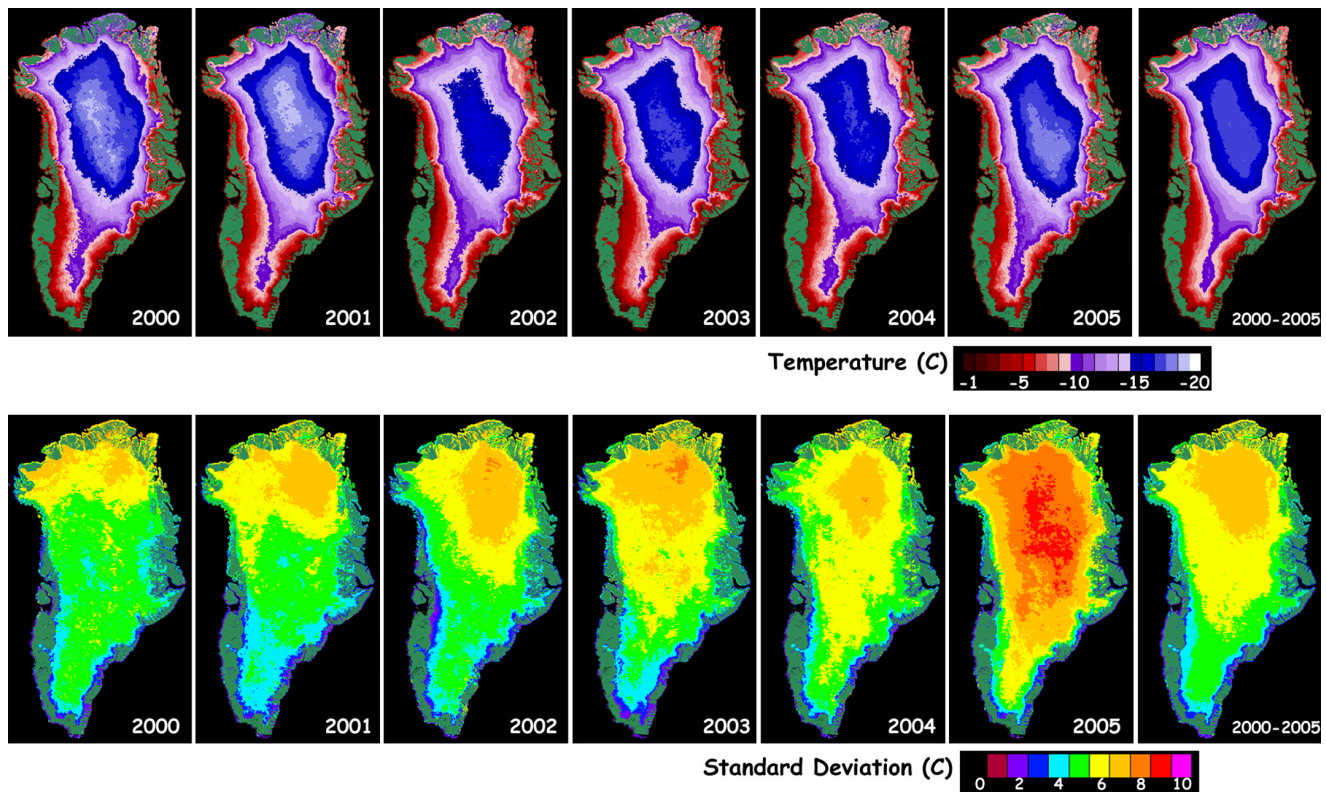


**Figure 2.** (top) Mean and (bottom) standard deviation (SD) MODIS land-surface temperature (LST) maps showing results of the melt season from April 30 or May 1 to September 28 or 29 (days 121–272) for each of the six years of the study (2000 to 2005); far right: six-year mean (top) and SD (bottom) maps. Base map is in the Albers conical equal-area projection. Land is shown in dark green around the edges of the ice sheet.

which is partly due to increased surface runoff, and this process has been observed to be advancing northward [Rignot and Kanagaratnam, 2006]. Air temperature and air-temperature changes would contribute to driving such processes.

[15] The boundaries between Benson’s dry-snow and percolation facies (the region on a glacier where snow and firn is subjected to localized percolation of meltwater without becoming wet throughout), and the ERS-1 synthetic-aperture radar (SAR)-derived dry-snow facies of Fahnestock *et al.* [1993] were digitally traced and overlaid on our 6-year mean SD map (Figure 3) to visualize the relationship between the glacier-facies boundaries (a function of ice-sheet mass balance), and surface-temperature

variability. This pattern suggests a correspondence with the glacier facies of Benson [1962], but especially with the SAR-derived dry-snow facies delineated by Fahnestock *et al.* [1993].

[16] This correspondence of high temperature variability and dry snow is likely because the thermal conductivity of dry snow is lower than that of wet snow. Air-temperature changes, induced by wind variability and weather patterns, are more likely to cause frequent surface-temperature changes in dry snow as compared to wet snow (with its higher thermal conductivity). Also, surface-temperature variability is lowest in the ablation area where the upper limit of surface temperature is 0°C. The glacier-facies boundaries can change over time with a change in mass

**Table 1.** Mean, Clear-Sky Surface Temperature (°C) and Standard Deviation (SD) of the Greenland Ice Sheet<sup>a</sup>

Year	Entire Melt	Number of Cells Used in the Calculation	Active-Melt	Number of Cells Used in the Calculation
	Season (Days 121–272): Mean LST and SD, °C		Season (Days 121–225): Mean LST and SD, °C	
2000	−11.45 ± 6.42	4,529,332	−10.27 ± 6.05	3,228,077
2001	−11.34 ± 6.56	4,160,062	−10.12 ± 5.82	2,878,232
2002	−9.94 ± 6.19	4,442,114	−8.29 ± 5.29	3,164,397
2003	−10.26 ± 6.64	4,429,452	−8.73 ± 5.43	3,170,990
2004	−10.48 ± 6.36	4,321,479	−8.61 ± 5.08	3,018,844
2005	−10.80 ± 7.55	4,484,320	−8.29 ± 5.43	3,181,810
All yrs.	−10.71 ± 6.66	26,366,759	−9.04 ± 5.59	18,642,348

<sup>a</sup>Temperatures and SDs are shown for the entire melt season from May through September (days 121–272) and for the period of most-active melt, from May through mid-August (days 121–225), each year.

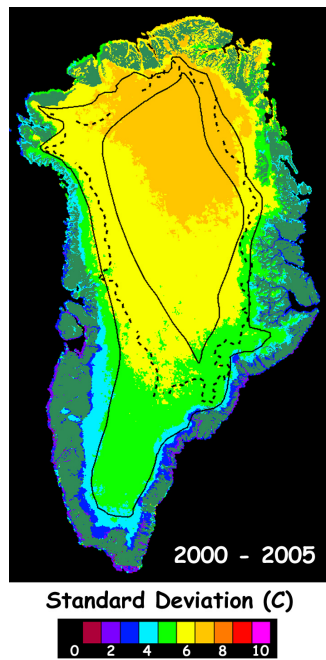


**Figure 3.** Six-year mean, land-surface temperature standard deviation map with the following lines superimposed: 1) solid black lines from *Benson* [1962]: outer boundary of the percolation facies, and inner - dry-snow facies boundary (or dry-snow line); 2) dashed black line represents dry-snow line derived from ERS-1 synthetic-aperture radar (SAR) [*Fahnestock et al.*, 1993]; original image from which SAR-derived, dry-snow line was drawn, was obtained from the National Snow and Ice Data Center in Boulder, Colorado.

balance driven by meteorological conditions such as air temperature and precipitation.

[17] We looked at the frequency of cloud cover during each melt season to ascertain whether or not the surface-temperature variability is an artifact caused by cloud-cover patterns. Though there is less cloud cover in northern vs. southern Greenland (Figure 1), there is no particular pattern in the cloud cover, thus indicating that the observed increasing surface-temperature variability is not an artifact of interannual cloud-cover variability.

## 5. Discussion and Concluding Remarks

[18] Higher ice-sheet surface temperatures can lead to enhanced ice-sheet disintegration when surface water percolates through great thicknesses of the ice sheet leading to an acceleration of ice-sheet flow [*Zwally et al.*, 2002]. We observed a general expansion of increasing surface-temperature variability from 2000 to 2005 on the Greenland Ice Sheet, being greatest in 2005, a year cited as being anomalously warm over Greenland by other investigators, and according to our LST data. The SDs are consistent with surface instability caused by air-temperature fluctuations.

[19] We also found that the two warmest years (2002 and 2005) are the same years that experienced the most-extensive melt of the six-year period. *Steffen et al.* [2004] showed that there was a very large melt extent in 2002, extending

over 690,000 km<sup>2</sup> of the ice sheet compared to a 1979–1999 average of 455,000 km<sup>2</sup> [*Abdalati and Steffen*, 2001], and 2005 has been cited by *Steffen and Huff* (<http://cires.colorado.edu/science/groups/steffen/greenland/melt2005/>) as experiencing melt equal or greater in area than occurred in 2002. This is consistent with the average melt-season LSTs presented herein, and findings by *Comiso* [2006] showing that those same two years were unusually warm using AVHRR data of the Arctic since 1981.

[20] MODIS-derived LST provides a quantitative assessment of the mean surface temperature and surface-temperature change on the Greenland Ice Sheet. Because the location of the glacier-facies boundaries reflects the ice sheet mass balance, a sustained increase in surface temperature would cause the glacier-facies boundaries to migrate to higher elevations.

[21] **Acknowledgments.** The authors thank Carl Benson of the University of Alaska, Long Chiu of George Mason University, and Waleed Abdalati and Christopher Shuman, of NASA/GSFC, and Konrad Steffen of CIRES for helpful discussions and/or reviews. Two anonymous reviewers provided further useful insights that led to significant improvements. Support for this work was provided by NASA's Earth Observing System and Cryospheric Sciences Programs.

## References

- Abdalati, W., and K. Steffen (1995), Passive microwave-derived snowmelt regions on the Greenland ice sheet, *Geophys. Res. Lett.*, *22*(7), 787–790.
- Abdalati, W., and K. Steffen (2001), Greenland ice sheet melt extent: 1979–1999, *J. Geophys. Res.*, *106*(D24), 33,983–33,989.
- Ackerman, S. A., K. I. Strabala, P. W. Menzel, R. A. Frey, C. C. Moeller, and L. E. Gumley (1998), Discriminating clear sky from clouds with MODIS, *J. Geophys. Res.*, *103*(D24), 32,141–32,157.
- Benson, C. S. (1962), Stratigraphic studies in the snow and firn of the Greenland ice sheet, *Res. Rep. 70*, 93 pp., U. S. Army Cold Reg. Res. and Eng. Lab., Hanover, N. H. (Reprinted and updated in 1996).
- Comiso, J. C. (2006), Arctic warming signals from satellite observations, *Weather*, *61*(3), 70–76.
- Comiso, J., J. Yang, S. Honjo, and R. A. Krishfield (2003), Detection of change in the Arctic using satellite and in situ data, *J. Geophys. Res.*, *108*(C12), 3384, doi:10.1029/2002JC001347.
- Fahnestock, M., R. Bindshadler, R. Kwok, and K. Jezek (1993), Greenland ice sheet surface properties and ice dynamics from ERS-1 SAR imagery, *Science*, *262*(5139), 1530–1534.
- Haefliger, M., K. Steffen, and C. Fowler (1993), AVHRR surface temperature and narrow-band albedo comparison with ground measurements for the Greenland ice sheet, *Ann. Glaciol.*, *17*, 49–54.
- Hall, D. K., A. T. C. Chang, J. L. Foster, C. S. Benson, and W. Kovalick (1989), Comparison of in-situ and Landsat-derived reflectances of Alaskan glaciers, *Remote Sens. Environ.*, *28*, 23–31.
- Hanna, E., P. Huybrechts, I. Janssens, J. Cappelen, K. Steffen, and A. Stephens (2005), Runoff and mass balance of the Greenland ice sheet: 1958–2003, *J. Geophys. Res.*, *110*, D13108, doi:10.1029/2004JD005641.
- Joshi, M., C. J. Merry, K. C. Jezek, and J. F. Bolzan (2001), An edge detection technique to estimate melt duration, season and melt extent on the Greenland ice sheet using passive microwave data, *Geophys. Res. Lett.*, *28*(15), 3497–3500.
- Key, J., and M. Haefliger (1992), Arctic ice surface temperature retrieval from AVHRR thermal channels, *J. Geophys. Res.*, *97*(D5), 5885–5893.
- Krabill, W., W. Abdalati, E. Frederick, S. Manizade, C. Martin, J. Sontag, R. Swift, R. Thomas, W. Wright, and J. Yungel (2000), Greenland ice sheet: High-elevation balance and peripheral thinning, *Science*, *289*, 428–430.
- Long, D. G., and M. R. Drinkwater (1999), Cryosphere applications of NSCAT data, *IEEE Trans. Geosci. Remote Sens.*, *37*(3), 1671–1684.
- Nghiem, S., K. Steffen, R. Kwok, and W.-Y. Tsai (2001), Detection of snowmelt regions on the Greenland ice sheet using diurnal backscatter change, *J. Glaciol.*, *47*(159), 547–593.
- Rignot, E., and P. Kanagaratnam (2006), Changes in the velocity structure of the Greenland Ice Sheet, *Science*, *311*, 986–990.
- Shuman, C. A., K. Steffen, J. E. Box, and C. R. Stearns (2001), A dozen years of temperature observations at the Summit: Central Greenland automatic weather stations 1987–99, *J. Appl. Meteorol.*, *40*, 741–752.

- Steffen, K., and J. Box (2001), Surface climatology of the Greenland ice sheet: Greenland climate network 1995–1999, *J. Geophys. Res.*, *106*(D24), 33,951–33,964.
- Steffen, K., S. V. Nghiem, R. Huff, and G. Neumann (2004), The melt anomaly of 2002 on the Greenland Ice Sheet from active and passive microwave satellite observations, *Geophys. Res. Lett.*, *31*, L20402, doi:10.1029/2004GL020444.
- Stroeve, J., and K. Steffen (1998), Variability of AVHRR-derived clear-sky surface temperature over the Greenland ice sheet, *J. Appl. Meteorol.*, *37*, 23–31.
- Wan, Z., Y. Zhang, Q. Zhang, and Z.-L. Li (2002), Validation of the land-surface temperature products retrieved from Terra Moderate Resolution Imaging Spectroradiometer data, *Remote Sens. Environ.*, *83*, 163–180.
- Williams, R. S., Jr., D. K. Hall, and C. S. Benson (1991), Analysis of glacier facies using satellite techniques, *J. Glaciol.*, *37*(125), 120–128.
- Zwally, H. J., W. Abdalati, T. Herring, K. Larson, J. Saba, and K. Steffen (2002), Surface melt-induced acceleration of Greenland ice-sheet flow, *Science*, *297*(5579), 218–222.
- 
- K. A. Casey and N. E. DiGirolamo, Science Systems and Applications, Inc., Lanham, MD 20706, USA.
- D. K. Hall, Cryospheric Sciences Branch, Code 614.1, NASA Goddard Space Flight Center, Greenbelt, MD 20771, USA. (dorothy.k.hall@nasa.gov)
- Z. Wan, Institute for Computational Earth System Science, University of California, Santa Barbara, CA 93106-3060, USA.
- R. S. Williams Jr., U.S. Geological Survey, Woods Hole Science Center, Woods Hole, MA 02543-1598, USA.